The power output and efficiency of a negative capacitance shunt for vibration control of a flexural system

Benjamin S. Beck, Kenneth Cunefare, Manuel Collet

The power output and efficiency of a negative capacitance shunt for vibration control of a flexural system

Benjamin S Beck[1], **Kenneth A Cunefare**[1] **and Manuel Collet**[2]

[1] G W Woodruff School of Mechanical Engineering, Georgia Institute of Technology, Atlanta, GA, USA

[2] FEMTO-ST, Department Applied Mechanics, Besanc¸on, France

Abstract

A negative capacitance shunt is a basic, analog, active circuit electrically connected to a piezoelectric transducer to control the vibrations of flexural bodies. The shunt circuit consists of a resistor and a synthetic negative capacitor to introduce a real and imaginary impedance on a vibrating mechanical system. The electrical impedance of the negative capacitance shunt modifies the effective modulus of the piezoelectric transducer to reduce the stiffness and increase the damping, which causes a decrease in amplitude of the vibrating structure to which the elements are bonded. To gain an insight into the electromechanical coupling and power output, the shunt and the electrical properties of the piezoelectric transducer are modeled using circuit modeling software. The power output of the model is validated with experimental measurements of a shunt connected to a piezoelectric transducer pair bonded to a vibrating aluminum cantilever beam. The model is used to select the passive components of the negative capacitance shunt to increase the efficiency and quantify the voltage output limit of the op-amp.

Nomenclature

(The subscripts 'p' and 'b' denote patch and beam, respectively.)

$E_{\mathrm{p}}^{\mathrm{SU}}$, E_{b}	Elastic modulus
C_i	Capacitor on branch i
C_{p}^{T}	Patch capacitance
I	Current
k_{31}	Electromechanical coupling coefficient
P	Real or active power
Q	Reactive power
R_i	Resistance on branch i
$\|S\|$	Apparent power
V	Voltage
Y^{SU}	Shunt admittance
$Z = \frac{1}{Y}$	Electrical impedance
Z_{in}	The input impedance of a circuit
ω	Angular frequency, rad s^{-1}

1. Introduction

Reduction in structural vibrations of flexural systems is desirable in many applications. A simple and effective way of controlling flexural vibrations is the use of shunted piezoelectric patches. Shunts are considered to be any electrical device that is connected between the two electrodes of a piezoelectric patch which has been bonded to a vibrating structure. There are many circuit designs which control or dampen structural motion, but this work will specifically focus on a negative capacitance shunt and how this circuit affects the electromechanical behavior of a flexural system. An investigation of the electrical power output of the shunt will be made using circuit modeling software[3] and validated experimentally. A comparison will then be made between the power output of the circuit and the amount of

[3] National Instruments Multisim.

suppression achieved by the shunt system on a vibration structure to determine the correlation between power output and suppression which will allow for better circuit design.

The use of electrical shunt circuits connected to a piezoelectric patch transducer bonded to a vibrating system was first investigated by Forward [1]. His work outlined the use of a shunt that used a resistor and inductor to generate an electrical resonance that was tuned to a structural mode to reduce the amplitude of vibration. His work was extended by Hagood and von Flotow, who recognized the link between the resonant shunt and a tuned mass absorber [2]. They also developed an equation which represents the modification of the elastic modulus of the piezoelectric material with the addition of any shunt admittance [2, 3],

$$E_{\mathrm{p}}^{\mathrm{SU}}(\omega) = E_{\mathrm{p}}^{E}\frac{\mathrm{i}\omega C_{\mathrm{p}}^{T} + Y^{\mathrm{SU}}}{\mathrm{i}\omega C_{\mathrm{p}}^{T}(1-k_{31}^{2}) + Y^{\mathrm{SU}}} \tag{1}$$

where Y^{SU} is the shunt admittance (the remainder of the equation's variables can be found in the Nomenclature). However, the control frequency bandwidth of a resonant shunt is limited to vibration modes at or near the electrical resonance [4–7]. Much research has been done on extending single mode shunts to multiple modes using a number of techniques [8–11]. Unfortunately, limitations such as the non-adaptive and experimentally cumbersome nature of these solutions are quite large. Therefore, other methods of creating broadband shunts are necessary.

A number of different adaptive, broadband control techniques have been developed that utilize a single piezoelectric element for both sensing and actuation. The first self-sensing broadband control shunt was introduced by Dosch [12]. This system uses a reference capacitor to estimate the voltage across the piezoelectric element that corresponds to the amount of strain on the vibrating structure. Other active self-sensing techniques utilize equation (1) to tailor a synthetic impedance to control the modulus of the piezoelectric element and reduce the vibration of a system over a wide frequency band [3, 13–15]. A specific, yet simple, synthetic impedance which exhibits broadband vibration control is the negative capacitance circuit [16–20]. A negative capacitance circuit is created from a single, active op-amp and a few passive circuit components. Although inherently a feedback control circuit [20], many researchers have described connecting a negative capacitance to a piezoelectric patch as a 'cancellation' or 'neutralizing' of the capacitance of the patch to increase the power dissipated in a resistor [17, 21, 22]. However, due to the sensitivity and instability of the negative capacitance circuit, measurement and quantification of the power within the shunt has been difficult to obtain. Therefore, an accurate electrical model of the piezoelectric-shunt system is necessary to fully describe the behavior and to improve the control efficiency of the shunt.

For the negative capacitance circuit to be considered a feasible control mechanism, the op-amp power versus some measure of control effort is required so that the requirements of the control system can be determined for controller design. Apart from a measurement of circuit power, the goal of this work is to describe increases in the efficiency of the shunt, which will be defined as the power output of the op-amp with respect to the impedance of the shunt. The electrical limitations of the shunt will also be quantified.

An efficiency discussion of a negative capacitance shunts has been made by Václavík and Mokrý for a piezoelectric stack actuator to decrease the force transmitted by a single degree of freedom piezoelectric oscillator at a single resonance [23]. However, they did not investigate how the power flow to the system was altered by changing the shunt parameters. The work at hand will discuss the change in efficiency over a large frequency range when utilizing the negative capacitance shunt for flexural control. The efficiency of the shunt will be defined as the power output of the shunt divided by the power supplied by the op-amp,

$$\eta = \frac{S_{\mathrm{shunt}}}{S_{\text{op-amp}}}. \tag{2}$$

However, for a desired negative capacitance shunt impedance to produce control, the power required by the shunt cannot change. Therefore, to increase the efficiency of the shunt, the power output of op-amp can be reduced through the selection of passive components for the negative capacitance element. To aid in this task, a piezoelectric patch connected to a negative capacitance shunt will be electrically modeled using circuit simulation software. The results of the numerical model will be validated with experimental measurements.

In the remainder of this paper, first a formulation of the implementation of a negative capacitance shunt is presented. Then, the circuit modeling is outlined, followed by the method used to obtain experimental data. We then present the results and analysis and close with our conclusions.

2. Negative capacitance shunt

The basis for the negative capacitance shunt is a negative impedance converter. A negative impedance converter is a classical circuit implementation of passive elements built around a single operational amplifier that produces a selectable negative impedance. Figure 1 shows a schematic of a negative impedance converter [24]. The circuit's input impedance created by the passive elements Z_2 through Z_4 is

$$Z_{\mathrm{in}} = -\frac{Z_3 Z_2}{Z_4} \tag{3}$$

where the impedance of the ith circuit element can be described as

$$Z_i = R_i + \left(\mathrm{i}\omega L_i + \frac{1}{\mathrm{i}\omega C_i}\right). \tag{4}$$

This work's investigations will be performed on a shunt which includes a circuit that produces negative capacitance, shown in figure 2. This circuit produces an input impedance of

$$Z_{\mathrm{in}} = -\frac{R_3}{R_4[\frac{1}{\mathrm{i}\omega C_2} + R_2]}. \tag{5}$$

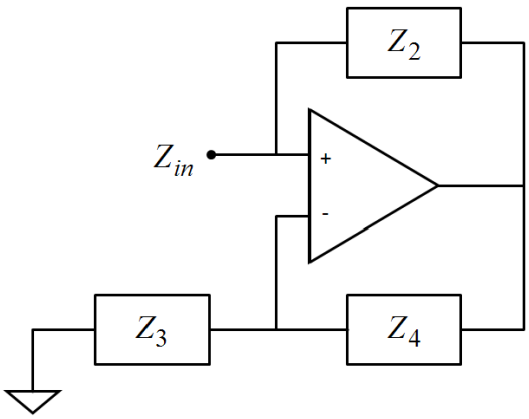

Figure 1. Schematic representation of a negative impedance converter.

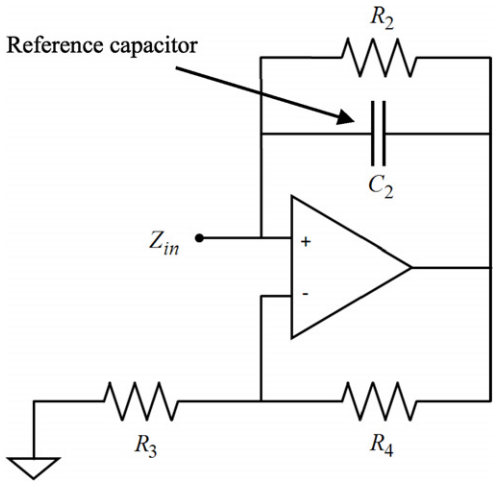

Figure 2. Negative capacitance circuit schematic.

The resistor R_2 is necessary for op-amp stability at DC, but is sufficiently large so as to be considered negligible, because for the configuration used here the real component of Z_{in} only appears below 10 Hz, which is below the frequencies of interest. Therefore, equation (5) can be simplified to

$$\frac{1}{\mathrm{i}\omega C_{\text{in}}} = \frac{1}{\mathrm{i}\omega C_2}\frac{R_3}{R_4}. \tag{6}$$

This can be rearranged to solve for the negative capacitance value

$$C_{\text{in}} = -\frac{R_4}{R_3}C_2 \tag{7}$$

where C_2 is considered the reference capacitor. The full shunt, figure 3, includes the negative capacitance element presented above and a resistor in series with the electrical model of a piezoelectric patch. The electrical model of the patch consists of a capacitor and a strain-induced voltage source. The magnitude of the voltage source is dictated by the amount of strain produced by the structure on which the patch is bonded. Therefore, for a typical system, this value will be strongly dependent on the frequency.

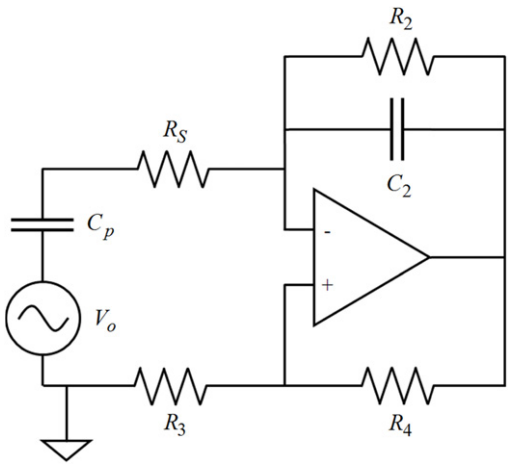

Figure 3. Full negative capacitance shunt schematic applied to a piezoelectric patch.

The total impedance of the shunt is

$$Z_{\text{sh}} = R_{\text{s}} + \frac{1}{\mathrm{i}\omega C_{\text{in}}}. \tag{8}$$

For experimental validation, the circuit is constructed around a TI-OPA445 operational amplifier. The adjustment of the negative capacitance is performed using a potentiometer for the resistance ratio R_4/R_3 in equation (7). The series resistor R_{s} is also a potentiometer to allow for straightforward, continuous adjustment. Note that figure 3 does not show all the circuit elements required to implement a robust, fully protected circuit for use as a negative capacitance shunt.

Figure 3 also leads to the calculation of the shunt power. Because the piezoelectric patch, series resistor, and negative capacitance element are all in series, the current within the loop can be calculated by

$$I_{\text{sh}} = \frac{V_{\text{o}}}{(\mathrm{i}\omega C_{\text{p}})^{-1} + Z_{\text{sh}}}. \tag{9}$$

Similarly, the voltage across the shunt is

$$V_{\text{sh}} = I_{\text{sh}} Z_{\text{sh}}. \tag{10}$$

Therefore, the power can be expressed in terms of the shunt impedance and the strain-induced voltage V_{o},

$$S_{\text{shunt}} = V_{\text{o}}^2 \frac{Z_{\text{sh}}}{[(\mathrm{i}\omega C_{\text{p}})^{-1} + Z_{\text{sh}}]^2}. \tag{11}$$

3. Circuit numerical modeling

The circuit model, shown in figure 4, is comprised of a piezoelectric patch connected to a negative capacitance shunt. With respect to the elements labeled in figure 4, the Multisim model includes the electrical equivalent model of a piezoelectric patch, which consists of a strain-induced voltage V_1 and a capacitor C_{p}. In contrast to figure 3, the model of the negative capacitance shunt includes all the necessary components for experimental implementation. The modeling software includes a manufacturer-provided electrical model

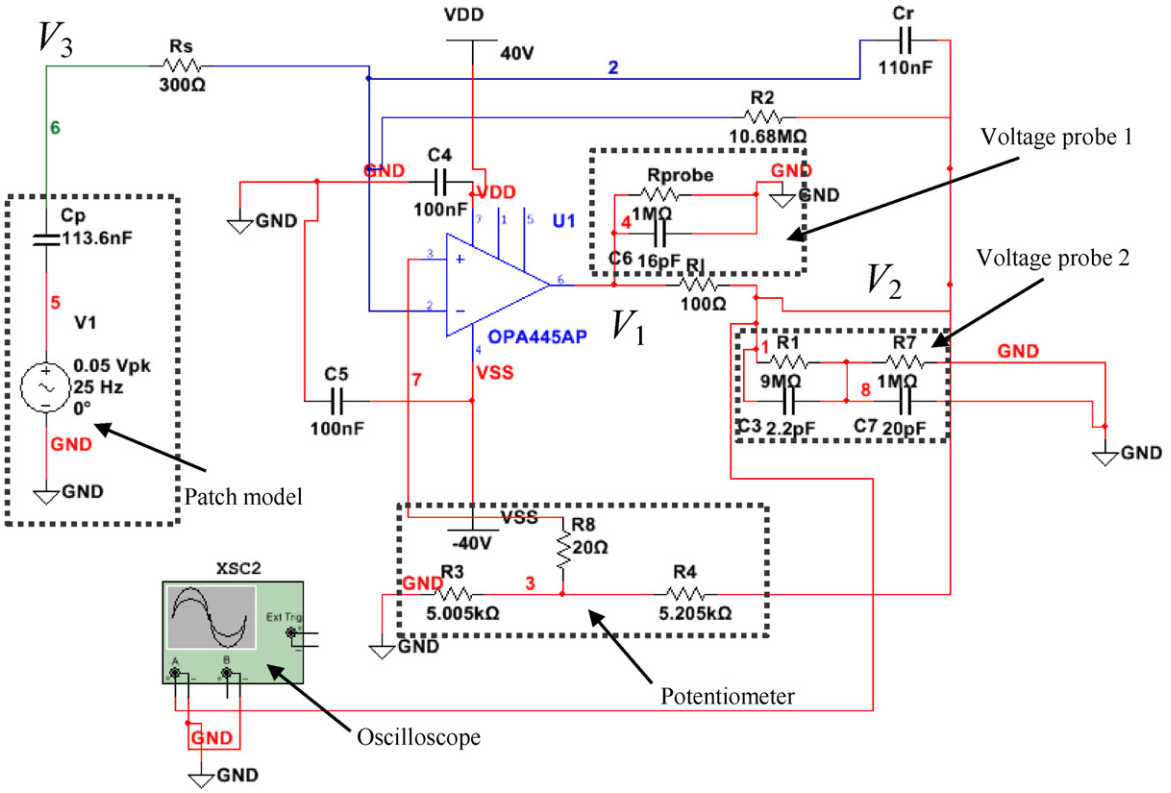

Figure 4. Shunt and patch circuit model.

of the op-amp to accurately simulate its electrical behavior. In addition to the shunt and patch, here we include the impedances of the two voltage sensors that are necessary to experimentally measure the circuit response. The current output of the op-amp is found by means of a voltage probe, voltage probe 1, measuring the voltage across a small resistor R_I to determine the current flowing through the output terminal of the op-amp. A separate voltage 10× voltage attenuation probe, voltage probe 2, is used to measure the op-amp output voltage, which is consistent with the probe used in experiments. A virtual oscilloscope is included in the model to measure the temporal response of the model. The software also performs AC circuit analyses to obtain frequency responses.

Generally, the imaginary component of impedance of the shunt is described as a single capacitance value for all frequencies, computed by the ratio approximation, equation (7). To demonstrate that the single negative capacitance value expression of the shunt is a valid representation of the shunt over the frequency range of interest, the ratio representation of the negative capacitance value is defined as

$$C_{\text{ratio}} = -\frac{R_4}{R_3} C_2 \tag{12}$$

where C_2 is the reference capacitor as shown in figure 2. For comparison, the impedance of the circuit model can be found by dividing the voltage of 'node 2', V_2, by the current through the series resistor R_s,

$$Z_{\text{sim}} = \frac{V_2}{R_s}, \tag{13}$$

where Z_{sim} is the simulated impedance. The effective capacitance of the negative capacitance circuit model can then be calculated by

$$C_{\text{sim}} = \frac{\text{Im}\,[Z_{\text{sim}}^{-1}]}{\omega} \tag{14}$$

where ω is the angular frequency. Figure 5 shows three frequency response plots of C_{sim} and the value of capacitance using the ratio representation C_{ratio}. The simulated response of the circuit closely matches that obtained through the simple ratio expression of equation (12) for all frequencies considered. The maximum error in capacitance between the two is 0.25%, therefore for frequencies from 10 to 5000 Hz the shunt can be accurately characterized by a single value of negative capacitance.

The power of shunt can also be calculated by

$$S_{\text{shunt}} = V_3 I_{R_s} \tag{15}$$

where V_3 is the total voltage across the full shunt as shown in figure 4 and I_{R_s} is the current through the series resistor R_3. This value will be used to calculate the efficiency of the shunt as defined by equation (2).

4. Experimental setup and procedure

Experiments to verify the electrical shunt model were performed on a cantilever beam, figure 6, with two pairs

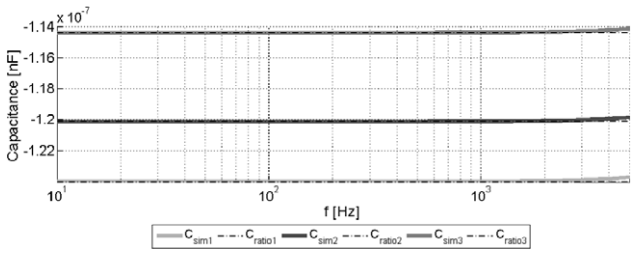

Figure 5. Simulated negative capacitance compared to the negative capacitance ratio representation.

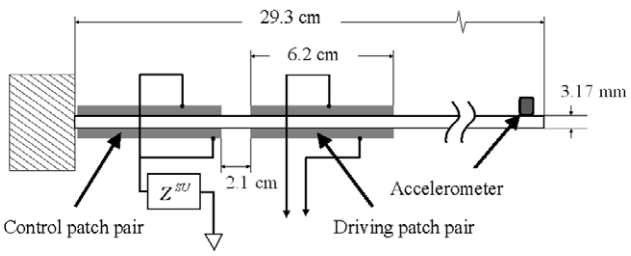

Figure 6. Cantilever beam with two pairs of piezoelectric patches.

Table 1. Beam and patch properties.

Beam	Young's modulus	$E_b = 73$ GPa
	Density	$\rho_b = 2700$ kg m^{-3}
	Width	$w = 2.55$ cm
Piezoelectric	Young's modulus, shorted	$E_p = 63$ GPa
	Density	$\rho_p = 7800$ kg m^{-3}
	Coupling coefficient	$k_{31} = 0.35$
	Thickness	$t = 0.25$ mm
	Capacitance, total	$C_p = 113$ nF

of piezoelectric patches bonded to the surface. One pair of patches is used to excite the beam. The pair of patches bonded near the root of the beam is utilized as the control patches. The physical properties of the beam and the patches used are in table 1. It has been previously shown that a negative capacitance shunt allows global reduction of the vibrations [16], therefore, for simplicity, a single accelerometer placed at the tip will be used to measure the response of the beam for various shunt conditions.

The method used to measure the electrical behavior of the shunt circuit during control of a cantilever beam is now outlined. The key electrical measure of interest is the power output of the operational amplifier. Figure 7 shows a schematic for the negative capacitance shunt for experimental validation with measurement probe locations. To find the output of the op-amp, the voltage at the output, V_2, is measured using a 10× attenuating voltage probe, and the current is measured by determining the voltage drop over a small resistor R_I placed at the output pin of the op-amp, shown in figure 7. The complex power output of the op-amp is computed by

$$S = [\bar{V}_2 I] \tag{16}$$

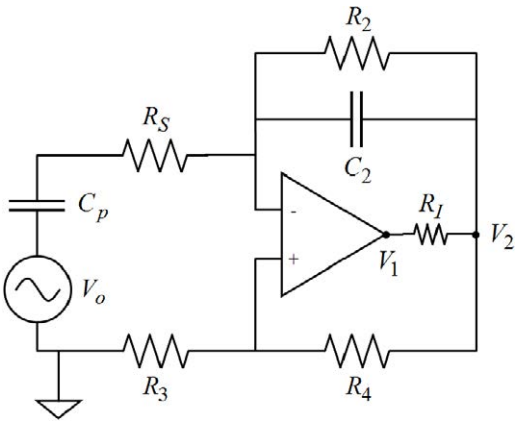

Figure 7. Full shunt circuit with measurement probe locations V_1 and V_2.

where the current is

$$I = \frac{V_I}{R_I} \tag{17}$$

and V_I is the voltage drop across resistor R_I

$$V_I = V_1 - V_2. \tag{18}$$

The complex power can be expressed in terms of its real and imaginary components,

$$S = P + \mathrm{i}Q \tag{19}$$

where P is the real power and Q is the reactive power. The apparent power is the magnitude of the complex power, $|S|$.

The responses of the beam and shunt circuit were acquired using a system consisting of a signal generator, the driving patches and a recording device to measure both the accelerometer and voltage responses of the beam and circuit. The beam was driven with a short sine sweep, or chirp, signal to excite frequencies from 10 to 5000 Hz. A Siglab system was used for both signal generation and data acquisition.

5. Results and analysis

The results and analysis are presented in three subsections. First, the circuit model is verified with experimentally obtained measurements of a negative capacitance shunt. Second, the efficiency of the shunt is explored by altering the passive components of the circuit and determining the power output of the op-amp. Finally, an investigation of the limitations of the op-amp utilized for the negative capacitance is presented.

5.1. Model verification

To verify the model, the power output of the op-amp, figure 7, was numerically simulated for four values of series resistance, R_s, and three values of negative capacitance, and compared to the measured power output. The circuit parameters used for verification in the circuit model and for the experiments are shown in table 2. The simulated power output for

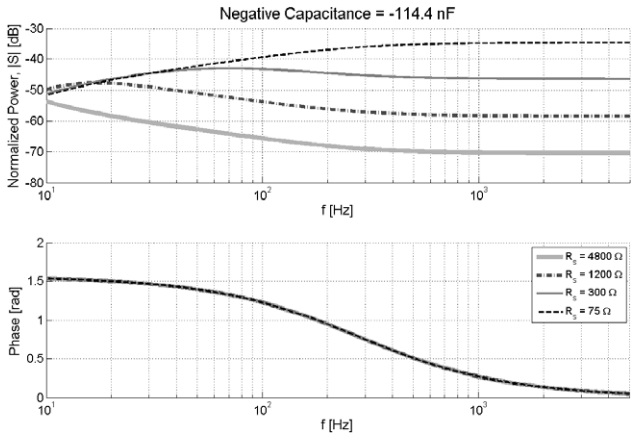

Figure 8. Simulated power output of the op-amp, amplitude and phase, for four values of series resistance.

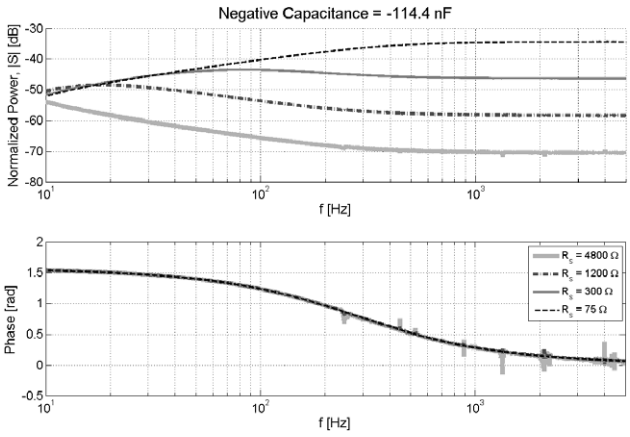

Figure 9. Normalized experimental power output of the op-amp, amplitude and phase, for four values of series resistance.

Table 2. Verification circuit parameters.

V_o	0.04 V
C_p	113.6 nF
C_2	110 nF
R_2	10.68 MΩ
$R_3 + R_4$	10.21 kΩ

four values of series resistance is shown in figure 8. The negative capacitance value of the shunt for all four resistors is −114.4 nF. At low frequencies, the power for all four cases is similar. However, the power output increases significantly for higher frequencies as the series resistance is reduced. An interesting result is that the phase of the power does not change for different resistance values, which indicates the series resistor only affects the bandwidth of the gain of the negative capacitance circuit but not the impedance of the negative capacitance element. Due to the resonances of the cantilever beam and the fact that the response of the beam is suppressed at different frequencies for the four series resistors, the model cannot be directly compared to the measured power output of the experimental circuit. Therefore, both the model solutions and experimental measurements of power must be normalized by some value which is dependent on the strain-induced voltage, which dictates the response of the circuit. Similarly, this value must be independent of the shunt parameters to allow power comparisons for different shunt configurations. Consequently, it was chosen to normalize the power output of the op-amp by the power of the piezoelectric patch if there were no shunt attached,

$$S_p = \frac{V_o^2}{i\omega C_p} \tag{20}$$

where V_o is the strain-induced voltage and C_p is the capacitance of the patch. The experimental normalized power output of the op-amp is shown in figure 9, which matches exactly with the output power magnitude and phase of the circuit model in figure 8.

The tip response of the beam is presented in figure 10. The tip response for the four resistance values of the negative

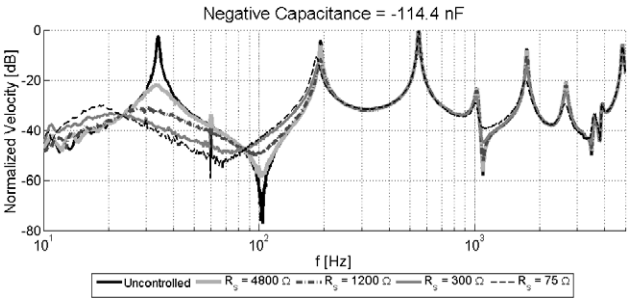

Figure 10. Tip response of the beam for four values of series resistance.

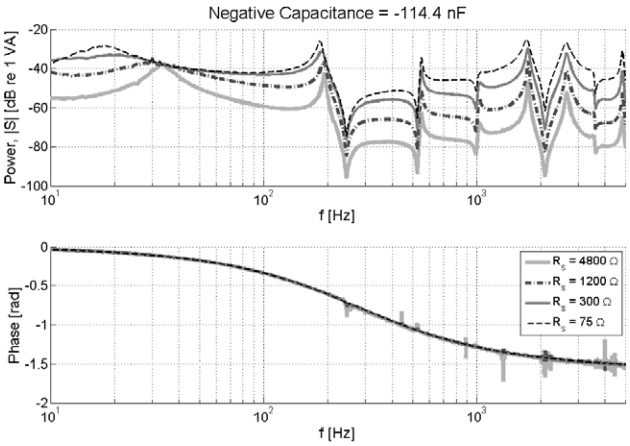

Figure 11. Experimental power output of the op-amp, amplitude and phase, for four values of series resistance.

capacitance shunt are shown along with the uncontrolled response. The series resistor alters how much suppression occurs at the resonances of the beam. For the first low-frequency resonances, at about 30 and 200 Hz, the 300 Ω resistor results in the greatest suppression, while the 75 Ω resistor improves the suppression at high-frequency resonances. Figure 11 shows the power output of the experimental circuit, which does not match the simulated power output. As stated above, the experimental response

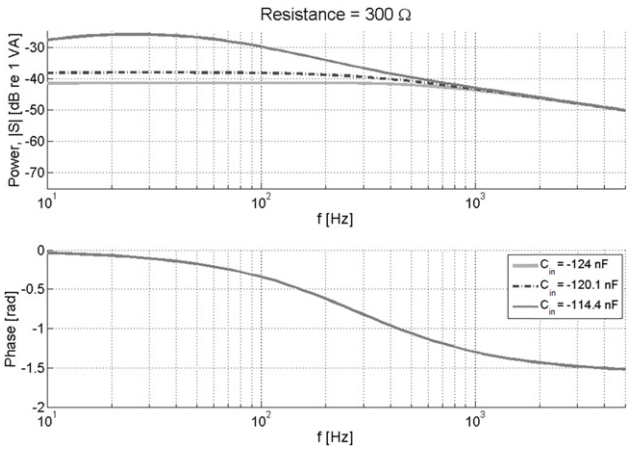

Figure 12. Simulated power output and phase of the op-amp for three values of negative capacitance.

Table 3. Total apparent (VA) power output of the op-amp for four resistor values, from 10 to 5000 Hz.

$R_s = 4800\ \Omega$	$R_s = 1200\ \Omega$	$R_s = 300\ \Omega$	$R_s = 75\ \Omega$
0.008	0.045	0.242	1.008

does not match the model due to the spectral variation of disturbance voltage caused by the resonant behavior of the beam. The phase of the power matches the numerical output exactly, and does not vary with change in resistor. It should be noted that a certain level of power output at a given frequency does not correspond to the same level of reduction in tip response. For example, the power output at 32 Hz is the exact same for all resistance values, but the response of the beam is drastically different. The total apparent power output of the op-amp for all frequencies is shown in table 3. Changing the resistor from 4800 to 75 Ω increases the total power by two orders of magnitude. However, the response of the beam for the 75 Ω resistor is greatly reduced compared to that observed with the 4800 Ω resistor. Therefore, more overall power output is necessary for more control over the entire frequency range of interest.

Figure 12 shows the simulated power output of the op-amp for three values of negative capacitance and a series resistor of 300 Ω. In contrast to changing the resistor, the change in negative capacitance has more effect on the power magnitude at low frequencies and no effect at high frequency. Again, the phase of the power is not affected by negative capacitance. The tip response of the cantilever beam, seen in figure 13, follows the trend of the simulated power output; whereby decreasing the negative capacitance magnitude, which raises the gain of the circuit, increases the suppression, especially at low frequencies. At high frequencies, there is no change in response on decreasing the negative capacitance magnitude. Figure 14 shows the measured power output of the op-amp. The power output does not change at high frequencies for different values of negative capacitance. The power output at low frequencies is reduced for some frequencies and increased for some

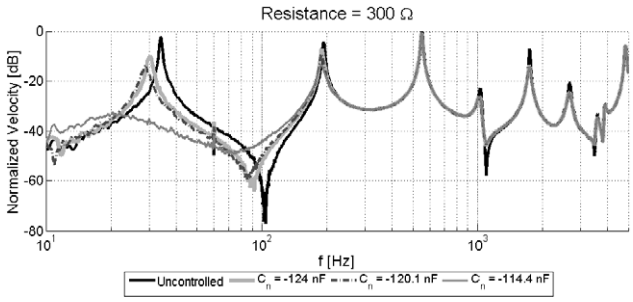

Figure 13. Tip response of the beam for three values of negative capacitance.

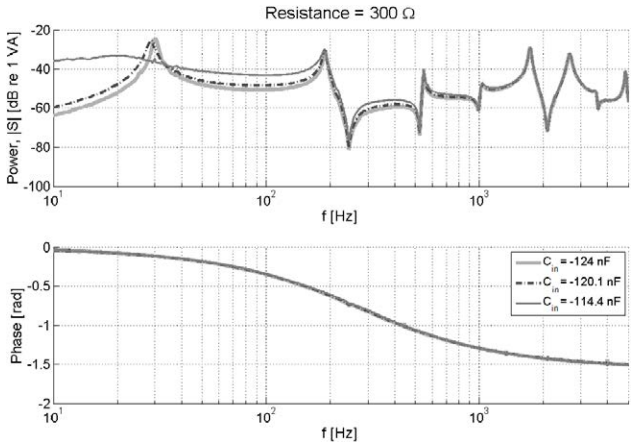

Figure 14. Experimental power output and phase of the op-amp for three values of negative capacitance.

Table 4. Total apparent power output (VA) of the op-amp for three negative capacitance values, from 10 to 5000 Hz.

$C_n = -124$ nF	$C_n = -120.1$ nF	$C_n = -114.4$ nF
0.185	0.203	0.242

frequencies. At the resonance, due to the reduction of the response, the power output is reduced but the power for frequencies off-resonance is increased. The phase of the power is consistent with the phase of the model. Table 4 shows the total measured power of the op-amp. The difference between the total output for the three negative capacitance values is much smaller than the difference by altering the resistors, as seen in table 3. Specifically, it requires only 30.8% more power for the circuit to reduce the first resonance by 23 dB by changing the negative capacitance from −124 to −114.4 nF. Therefore, it takes substantially less power to decrease low-frequency resonances by decreasing the negative capacitance than decreasing high-frequency resonances by reducing the resistor.

5.2. Efficiency improvements

As shown above, the circuit model accurately predicts the power output behavior of a negative capacitance shunt, apart from resonance behavior. Therefore, it can be used to

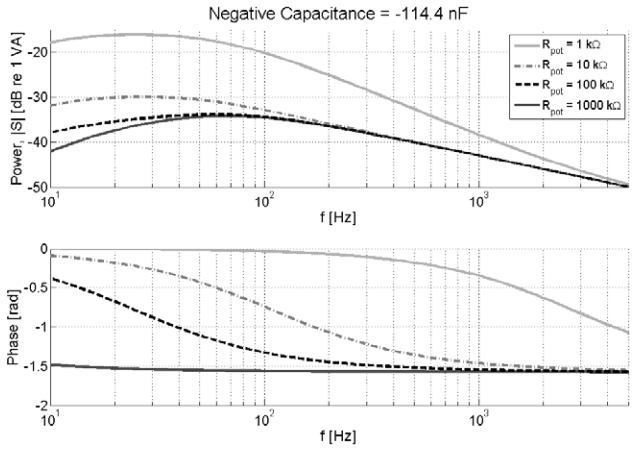

Figure 15. Simulated power output versus frequency for four potentiometer values.

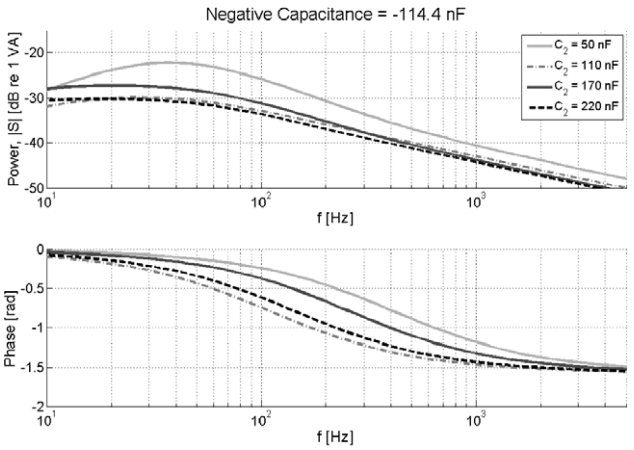

Figure 16. Simulated power output versus frequency for four reference capacitor values.

investigate how the choice in circuit parameters can increase the efficiency of the shunt by reducing the power output of the op-amp. Through inspection of equation (11) and the fact that the magnitude of the passive components of the negative capacitance element can be altered without changing the impedance, the efficiency can only be increased by reducing the power output of the op-amp. Qualitatively, since the impedance desired is a negative capacitor, the phase of the power should be close to $-\pi/2$ rad, which is the phase of power for an ideal negative capacitor. Also, because of the fact that the phase of the power is not affected by the negative capacitance value or series resistor, the passive components used to create the negative capacitance will be analyzed to increase the efficiency of the shunt.

To achieve a desired impedance with the negative capacitance shunt using equation (12), the design space for choice of circuit elements is quite large. However, the choice of circuit elements affects the power output of the shunt. This is illustrated in figure 15, which shows the power output of the op-amp versus the total potentiometer resistance in the positive leg of the circuit

$$R_{\text{pot}} = R_3 + R_4 \tag{21}$$

for a single negative capacitance value and series resistance, and considering four values for R_{pot}. The power output of the op-amp changes significantly with the value of R_{pot}. The 100 kΩ potentiometer has the smallest op-amp power output for this system. The phase of the power for that potentiometer is also the closest to that of the ideal negative capacitor. Therefore, the negative capacitance circuit will obtain maximum efficiency at a given optimal potentiometer resistance. Similarly, the power output for four values of reference capacitance C_2 is shown in figure 16. The reference capacitor does not change the power output of the op-amp as much as the potentiometer. However, for this system a 110 nF reference capacitor results in power output of the op-amp, with a phase that is closest to $-\pi/2$ rad for all frequencies. The 220 nF capacitor has slightly less power output for most frequencies. Therefore, generally, power output efficiency will be increased by a reference capacitor equal to the patch capacitance, but the optimal potentiometer must be computed for.

5.3. Circuit limitations

Because the model includes an accurate representation for op-amp behavior, the limitations of the shunt can be determined. During operation, the op-amp voltage and current are limited by the op-amp power supply and specifications. An analysis of the voltage output is presented here, but a similar investigation can be performed for the current limitations. For a constant amplitude disturbance voltage, the frequency at which the op-amp voltage is at a maximum is where the series resistance equals the real part of the negative impedance, where the negative impedance is

$$Z_2 = \frac{R_3}{R_4}\left[\frac{1}{R_2} + \mathrm{i}\omega C_2\right]^{-1}. \tag{22}$$

Due to the fact that a large resistor is chosen for R_2 and R_s is small, the maximum voltage occurs at low frequency. Figure 17 shows the low-frequency voltage output of the op-amp for four values of series resistance. The frequency at which the maximum occurs moves to higher frequencies for smaller values of resistance. The amplitude of the maximum is the same for all values of series resistance. The magnitude of the peak voltage value is determined by the negative capacitance value, as shown by figure 18. The maximum voltage increases as the negative capacitance decreases. However, the increase is nonlinear. The voltage peak increases exponentially as the negative capacitance magnitude approaches the simulated patch capacitance C_p. Therefore, the voltage response of the op-amp is sensitive to changes in negative capacitance near the patch capacitance.

The AC analysis makes linear, harmonic assumptions to determine the circuit response. However, the circuit response becomes nonlinear as the voltage output approaches the op-amp power supply voltage because of the voltage output limit of the op-amp. The nonlinearity of the voltage output can be seen in figure 19. The voltage response versus time for

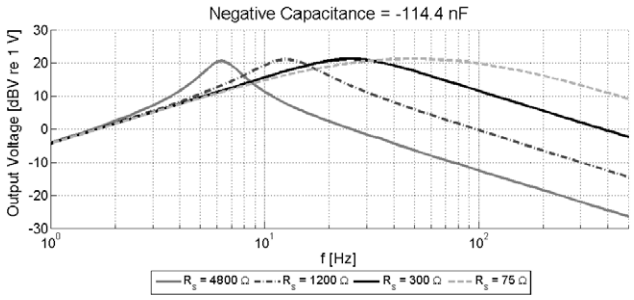

Figure 17. Low-frequency simulated voltage output versus frequency for four potentiometer values.

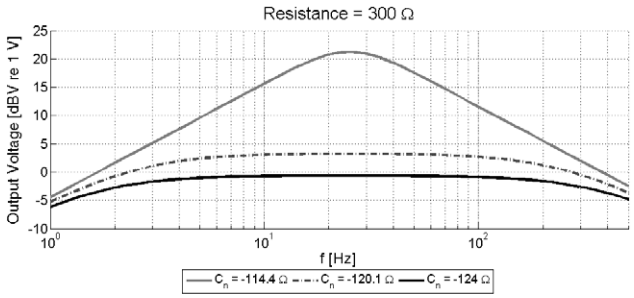

Figure 18. Low-frequency simulated voltage output versus frequency for three negative capacitance values.

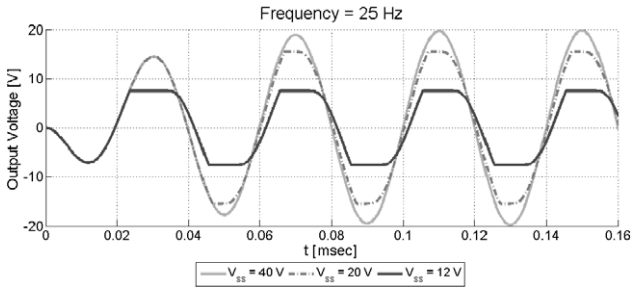

Figure 19. Op-amp voltage output for three values of power supply voltage.

a single frequency is shown for three values of power supply voltage V_{ss}. For a 40 V power supply, the circuit behaves normally, but as the power supply voltage is reduced, the amplitude of the response is decreased due to clipping. For the 12 V supply, the response mimics that of an unstable circuit, even though the circuit parameters allow a stable response for the 40 V supply. Therefore, when a negative capacitance shunt is to be applied on a system, a circuit model should be used to determine the parameters and supply voltage that can be implemented for a given shunt to achieve a linear response for a given disturbance.

6. Conclusion

A modeling approach to determine the power output and efficiency of a negative capacitance shunt was presented and confirmed. It was shown that a circuit model of a piezoelectric patch connected to a negative capacitance shunt accurately predicts the power output of the op-amp. Model investigations showed that by selection of the passive elements of a negative capacitance inverter, the efficiency of the shunt can be increased with a optimal potentiometer and a reference capacitor with equal capacitance as the piezoelectric transducer. Also, the model can predict the voltage output limits of the op-amp for the ratio of disturbance voltage to op-amp supply voltage.

References

[1] Forward R L 1979 Electronic damping of vibrations in optical structures *Appl. Opt.* **18** 690–7

[2] Hagood N W and von Flotow A 1991 Damping of structural vibrations with piezoelectric materials and passive electrical networks *J. Sound Vib.* **146** 243–68

[3] Park J and Palumbo D L 2004 A new approach to identify optimal properties of shunting elements for maximum damping of structural vibration using piezoelectric patches *Active 2004 (Williamsburg, VA)*

[4] Wu S-Y 1996 Piezoelectric shunts with a parallel *R–L* circuit for structural damping and vibration control *SPIE—Smart Structures and Materials 1996 (Newport Beach, CA)* pp 259–69

[5] Hollkamp J J and Gordon R W 1996 An experimental comparison of piezoelectric and constrained layer damping *Smart Mater. Struct.* **5** 715–22

[6] Caruso G 2001 A critical analysis of electric shunt circuits employed in piezoelectric passive vibration damping *Smart Mater. Struct.* **10** 1059–68

[7] Spadoni A, Ruzzene M and Cunefare K 2009 Vibration and wave propagation control of plates with periodic arrays of shunted piezoelectric patches *J. Intell. Mater. Syst. Struct.* **20** 979–90

[8] Hollkamp J J 1994 Multimodal passive vibration suppression with piezoelectric materials and resonant shunts *J. Intell. Mater. Syst. Struct.* **5** 49–57

[9] Wu S-Y 1998 Method for multiple mode piezoelectric shunting with single PZT transducer for vibration control *J. Intell. Mater. Syst. Struct.* **9** 991–8

[10] Behrens S, Moheimani S O R and Fleming A J 2003 Multiple mode current flowing passive piezoelectric shunt controller *J. Sound Vib.* **266** 929–42

[11] Niederberger D, Fleming A, Moheimani S O R and Morari M 2004 Adaptive multi-mode resonant piezoelectric shunt damping *Smart Mater. Struct.* **13** 1025–35

[12] Dosch J J, Inman D J and Garcia E 1992 A self-sensing piezoelectric actuator for collocated control *J. Intell. Mater. Syst. Struct.* **3** 166–85

[13] Moheimani S O R, Fleming A J and Behrens S 2003 On the feedback structure of wideband piezoelectric shunt damping systems *Smart Mater. Struct.* **12** 49–56

[14] Fleming A J and Moheimani S O R 2003 Adaptive piezoelectric shunt damping *Smart Mater. Struct.* **12** 36–48

[15] Quaegebeur N, Micheau P and Berry A 2009 Decentralized harmonic control of sound radiation and transmission by a plate using a virtual impedance approach *J. Acoust. Soc. Am.* **125** 2978–86

[16] Beck B, Cunefare K A and Ruzzene M 2008 Broadband vibration suppression assessment of negative impedance shunts *SMASIS08 (Ellicott City, MD)*

[17] Park C H and Baz A 2005 Vibration control of beams with negative capacitive shunting of interdigital electrode piezoceramics *J. Vib. Control* **11** 331–46

[18] Wu S-Y 2001 Broadband piezoelectric shunts for passive structural vibration control *SPIE—Smart Structures and Materials 2001 (Newport Beach, CA)* pp 251–61

[19] Cunefare K A 2006 Negative capacitance shunts for vibration suppression: wave based tuning and reactive input power *Active 2006 (Adelaide)*
[20] Behrens S, Fleming A J and Moheimani S O R 2001 New method for multiple-mode shunt damping of structural vibration using a single piezoelectric transducer *SPIE—Smart Structures and Materials 2001 (Newport Beach, CA)* pp 239–50
[21] Tang J and Wang K W 2001 Active-passive hybrid piezoelectric networks for vibration control: comparisons and improvement *Smart Mater. Struct.* **10** 794–806
[22] Bisegna P 2005 On the use of negative capacitances for vibration damping of piezoactuated structures *Proc. SPIE* **5760** 317–28
[23] Václavík J and Mokrý P 2012 Measurement of mechanical and electrical energy flows in the semiactive piezoelectric shunt damping system *J. Intell. Mater. Syst. Struct.* **23** 527–33
[24] Horowitz P and Hill W 1996 *The Art of Electronics* (New York, NY: Cambridge University Press)